THE ASTROPHYSICAL JOURNAL, 276:454–465, 1984 January 15

MULTIFREQUENCY OBSERVATIONS OF THE BL LACERTAE OBJECT 0735+178

J. N. BREGMAN, A. E. GLASSGOLD, AND P. J. HUGGINS
New York University

H. D. ALLER, M. F. ALLER, AND P. E. HODGE
University of Michigan Radio Observatory

G. H. RIEKE AND M. J. LEBOFSKY
Steward Observatory, University of Arizona

J. T. POLLOCK, A. J. PICA, R. J. LEACOCK, A. G. SMITH, AND J. WEBB
Rosemary Hill Observatory, University of Florida

T. J. BALONEK, W. A. DENT, AND C. P. O'DEA
University of Massachusetts

W. H.-M. KU
Columbia Astrophysics Laboratory, Columbia University

D. A. SCHWARTZ
Center for Astrophysics

J. S. MILLER
Lick Observatory, University of California, Santa Cruz

AND

R. J. RUDY AND P. D. LEVAN
Center for Astrophysics and Space Science, University of California, San Diego
Received 1983 January 24; accepted 1983 June 17

ABSTRACT

Four simultaneous spectra covering the radio through the X-ray regimes were made between 1979 October and 1981 March of the variable BL Lac object 0735+178. In each spectrum, the IR-UV synchrotron continuum dominates the total observed power (10^{47} ergs s^{-1}) and presumably becomes opaque between 10^{11} and 10^{13} Hz. A comparison of the spectra shows that the IR-UV flux changed dramatically (up to 380%), the radio flux changed modestly (8%–40%), and the X-ray flux varied modestly, if at all (<50%). Extensive nonsimultaneous observations were made over a longer period of time in order to study long- and short-term variability at X-ray, optical, and radio frequencies. These data show that the rapid and dramatic variations evident at infrared and optical wavelengths are absent at radio and X-ray frequencies. These observations support a picture where the IR-UV flux emanates from a small region, while the X-rays are produced by the inverse Compton process in the radio-emitting region (partly opaque synchrotron emission gives rise to the radio flux). By using existing VLBI data and theoretical arguments, we estimate that the IR-UV emission comes from a region approximately 5×10^{16} cm in radius, with a magnetic field of ~ 10 gauss, a density factor of $k \sim 10^6$ cm^{-3}, and a mass of 10^{-3} $M_\odot$. The particles, photons, and magnetic field may not be far from equipartition in this region. The radio and X-ray emission come from a larger region (10^{18}–10^{20} cm) of lower magnetic field ($\sim 10^{-3}$ G), comparable density parameter (10^4–10^6 cm^{-3}), and greater mass ($\sim 10^3$ $M_\odot$). Here, the energy density of the particles is dominant.

In the process of this analysis, we develop strong theoretical arguments regarding the radial behavior of the electron density and magnetic field.

Subject headings: BL Lacertae objects — infrared: sources — radiation mechanisms — radio sources: variable — X-rays: sources

I. INTRODUCTION

A central issue of quasar research is to develop a clear understanding of the conditions in the continuum-emitting region. Here, we address this problem by exploiting the usefulness of time-frozen multifrequency spectra of the violently variable BL Lac object 0735+178.

Because of instrumental and observational limitations, observations of BL Lac objects and quasars fall into one of three separate frequency regimes: radio ($<10^{11}$ Hz), IR-UV ($10^{13.5}$–$10^{15.5}$ Hz), and X-rays (10^{17}–10^{18} Hz). The rapid variability of BL Lac objects demands that simultaneous observations be obtained in order to compare critically the emission properties of these separate spectral regions. As an ongoing program, we regularly obtain simultaneous multifrequency spectra of a variety of BL Lac objects and violently variable quasars. Analyses of the X-ray bright BL Lac object I Zw 187, the red quasar 1413+135, and the flaring quasar 1156+295 are presented elsewhere (Bregman *et al.* 1981, 1982; Glassgold *et al.* 1983). Here we report on several multifrequency spectra of the luminous BL Lac object 0735+178 taken between 1979 October and 1981 March. From these spectra, and complementary data, we demonstrate the existence of several emitting regions, identify the dominant radiation process in each region, and calculate the physical conditions therein.

The source 0735+178 shows all the properties of the BL Lac class of objects. It is rapidly variable, has a high degree of optical polarization, and lacks emission lines. Optical variations of 0735+178, first detected by Wing (1973) and Carswell *et al.* (1974), are typical of BL Lac objects, showing short-term burstlike activity superposed on a more slowly varying component. The time scale for variability, defined as $|dt/d(\ln F_\nu)|$ throughout this paper, is frequently found to be less than a week (Pollock 1982). Measurements in B have been recorded as bright as 13.90 mag and as faint as 17.22 mag (Pollock *et al.* 1979).

Even within the class of BL Lac objects, 0735+178 is distinguished by certain optical and infrared polarization properties. Its unusually high degree of polarization (>30% at times; Angel and Stockman 1980) is wavelength dependent (greater polarization at shorter wavelength), and its infrared polarization and flux changes are correlated in the sense that the polarization decreases as the flux rises (Rieke *et al.* 1977; Puschell and Stein 1980; Impey *et al.* 1982). Like other high-luminosity objects, the angle of polarization is not restricted to a narrow range, and large day-to-day variations are observed in the degree and angle of polarization (Angel and Stockman 1980). While the high degree of polarization argues strongly for a synchrotron origin for the emission, the detailed physical basis for the various polarization properties is not fully understood.

The radio fluxes are also polarized and variable, but to a lesser extent than the optical fluxes (Balonek 1982; Perley 1982). The most unusual aspect of the radio spectrum is its flatness from frequencies below 1 GHz to the highest observable frequency at 90 GHz. VLBI observations at different frequencies reveal several components of different sizes that conspire to produce this flat spectrum (Cotton *et al.* 1980; Marscher and Shaffer 1980; Bååth *et al.* 1981). The most detailed VLBI map, made at 5 GHz, shows that most of the flux comes from an unresolved core (<0.3 milli-arcsec [mas]), part comes from a 1.22 mas region that is 4.2 mas from the unresolved core, and the remaining flux (~20%) comes from two larger regions (Bååth *et al.* 1981), both of which are less than 300 mas (Ulvestad, Johnston, and Weiler 1982). Observations in progress (Bååth *et al.* 1983) will determine whether "superluminal" motion exists between any of these components.

Although the absence of emission lines prevents us from determining the distance to 0735+178 in the usual way, a prominent absorption-line redshift system at $z = 0.424$ (Carswell *et al.* 1974) sets a lower limit to its distance. Additional absorption-line systems, common in objects with $z > 1.5$ (Weymann *et al.* 1979; Sargent *et al.* 1980), are not observed in this bright object, suggesting that $z < 1.5$. Also, most of the quasars listed in the Hewitt and Burbidge (1980) quasar catalog with absorption-line redshifts of $z < 1$ have almost identical emission- and absorption-line redshifts. Therefore, in the absence of a better estimate, we shall assume that the redshift of 0735+178 is 0.424.

Multifrequency spectra of 0735+178 and variability data are presented in § II. In § III we discuss the temporal flux variations, the multifrequency spectra, the connection to the VLBI data, and suggest a picture of the emitting regions. Modeling is used to develop further this picture and give it a quantitative foundation (§ IV); the conclusions are presented in § V.

II. OBSERVATIONS

Observations were obtained from 10^9 to 10^{18} Hz during four observing epochs from 1979 October to 1981 March using 11 different telescopes. The data are summarized in Table 1 and Figures 1 and 2, and are discussed below as a function of decreasing frequency.

a) Absorbing Material

Because 0735+178 lies at $b = 18°$ and has a known absorption-line system at $z = 0.424$, corrections to the observations must be made for absorption by galactic and extragalactic gas. Ultraviolet observations of the Lyα line and the Lyman discontinuity at $z = 0.424$ require the column density of neutral hydrogen to be less than 2×10^{19} cm^{-2} (Bregman, Glassgold, and Huggins 1981). This gas, which is characterized by low-excitation absorption lines (Boksenberg, Carswell, and Sargent 1979), has a column density too low to produce noticeable absorption in the soft X-ray band (0.25–4 keV) or at energies below 1 rydberg. The H I column density within our Galaxy toward 0735+178 is approximately 6.5×10^{20} cm^{-2} (Tolbert 1972; Heiles 1975), which gives rise to a reddening of 0.05 ± 0.03 (Burstein and Heiles 1978). For the remainder of this paper, we adopt $E(B-V) = 0.05$ and correct the optical and ultraviolet data according to the reddening law described by Seaton (1979).

b) X-Ray Observations

As part of larger programs at Columbia Astrophysics Lab (CAL) and the Center for Astrophysics (CFA), 0735+178 was observed with the imaging proportional counter on the *Einstein Observatory* 22 times between 1979 October and 1981 March. The X-ray data that comprise part of the simultaneous spectra are listed in Table 1, and all existing X-ray observations are listed in Table 2. Fluxes were obtained by using a column density for instrumental absorption of 5×10^{20} cm^{-2} and a power-law energy index of -1.0. The monochromatic and integrated fluxes are subject to systematic uncertainties that arise from calibration difficulties in the IPC; the systematic error is approximately 30% (2 σ).

No evidence of variability has been found in any of the CAL data or in any of the CFA data. When fast Fourier analysis was applied to the CAL data, no periodicities or non-Poisson behavior in the flux were found on any time scale. One sigma upper limits on the order of 30% can be set for variability on time scales longer than a few hundred seconds.

The accurate determination of spectral parameters from the IPC is still difficult because of calibration problems. We have compared the data obtained orbit-by-orbit and found no changes in the spectral distribution. The hardness ratio (Zamorani *et al.* 1981) is approximately 1.0, which is near the median found for quasars and implies a spectral slope of approximately -0.5.

TABLE 1

MULTIFREQUENCY OBSERVATIONS OF 0735+178

Observer	Date (year/month/day)	Region	Observing Band	Raw Data	logν(Hz)	$\log F_\nu$ (ergs cm^{-2}s^{-1}Hz^{-1})
Ku	79/10/19.1	X-Ray(IPC)	0.5-3.5 keV	0.057±0.007 cts/s[1]	17.38	-29.55±0.08[1]
Schwartz	80/10/9.1	X-Ray(IPC)	0.5-3.5 keV	0.054±0.004 cts/s	17.38	-29.47±0.07
	81/3/26.8		0.5-3.5 keV	0.050±0.005 cts/s	17.38	-29.57±0.07
Bregman, Glassgold and Huggins	79/10/19.1	UV(IUE)	1335-1435Å	2.81 (-15)[2]	15.336	-26.57±0.05
			1435-1535Å	2.68 (-15)	15.305	-26.54±0.05
			1535-1635Å	3.03 (-15)	15.277	-26.44±0.05
			1635-1735Å	3.16 (-15)	15.250	-26.37±0.05
			1735-1835Å	3.11 (-15)	15.225	-26.33±0.05
			1835-1935Å	2.80 (-15)	15.202	-26.32±0.05
	79/10/19.0	UV(IUE)	1900-2410Å	2.02 (-15)	15.144	-26.29±0.07
			2515-2760Å	2.79 (-15)	15.056	-26.06±0.04
			2760-3005Å	2.78 (-15)	15.017	-26.00±0.05
			3005-3250Å	2.68 (-15)	14.982	-25.94±0.05
	80/10/8.2	UV(IUE)	1320-1425Å	1.24 (-14)	15.339	-25.94±0.04
			1425-1530Å	1.27 (-14)	15.307	-25.87±0.04
			1530-1635Å	1.19 (-14)	15.278	-25.85±0.04
			1635-1740Å	1.12 (-14)	15.250	-25.82±0.04
			1740-1845Å	1.17 (-14)	15.224	-25.74±0.04
			1845-1950Å	1.05 (-14)	15.199	-25.74±0.04
	80/10/9.3	UV(IUE)	1320-1425Å	1.25 (-14)	15.339	-25.93±0.04
			1425-1530Å	1.37 (-14)	15.307	-25.83±0.05
			1530-1635Å	1.27 (-14)	15.278	-25.81±0.05
			1635-1740Å	1.22 (-14)	15.250	-25.78±0.05
			1740-1845Å	1.26 (-14)	15.224	-25.73±0.04
			1845-1950Å	1.12 (-14)	15.199	-25.71±0.04
	80/12/6.3	UV(IUE)	1320-1425Å	6.34 (-15)	15.339	-26.23±0.04
			1425-1530Å	5.95 (-15)	15.307	-26.20±0.04
			1530-1635Å	6.05 (-15)	15.278	-26.14±0.05
			1635-1740Å	5.59 (-15)	15.250	-26.12±0.05
			1740-1845Å	5.18 (-15)	15.224	-26.10±0.04
			1845-1950Å	5.69 (-15)	15.199	-26.00±0.04
Miller	80/10/9.5	Optical	3450-3950Å	7.20 (-15)[2]	14.909	-25.39±0.01
			3950-4450Å	7.02 (-15)	14.854	-25.30±0.01
			4450-4950Å	6.57 (-15)	14.805	-25.24±0.01
			4950-5450Å	6.14 (-15)	14.761	-25.19±0.01
			5450-5950Å	6.04 (-15)	14.721	-25.12±0.01
			5950-6450Å	5.47 (-15)	14.685	-25.10±0.01
			6450-6950Å	5.30 (-15)	14.651	-25.05±0.01
			6950-7450Å	5.10 (-15)	14.620	-25.01±0.01
Pollock, Pica, Smith, and Webb	80/10/9.3	Optical	U	14.33±0.10	14.92	-25.39±0.04
			B	15.06±0.10	14.83	-25.29±0.04
			V	14.36±0.10	14.74	-25.18±0.04
			I_k	13.62±0.13	14.56	-24.99±0.05
	80/12/6.3	Optical	U	14.68±0.10	14.92	-25.54±0.04
			B	15.27±0.08	14.83	-25.37±0.03
			V	14.78±0.08	14.74	-25.29±0.03
			I_k	14.03±0.16	14.56	-25.16±0.06

TABLE 1—*Continued*

MULTIFREQUENCY OBSERVATIONS OF 0735+178

Observer	Date (year/month/day)	Region	Observing Band	Raw Data	$\log\nu$ (Hz)	$\log F_\nu$ (ergs $cm^{-2} s^{-1} Hz^{-1}$)
	81/3/26.0	Optical	U	14.76±0.10	14.92	-25.57±0.04
			B	15.41±0.10	14.83	-25.43±0.04
			V	15.18±0.10	14.74	-25.45±0.04
			I_k	14.47±0.16	14.56	-25.33±0.06
Rudy and LeVan	79/10/20.4	Infrared	J	13.72±0.18	14.38	-25.29±0.07
			H	13.13±0.10	14.26	-25.23±0.04
			K	12.25±0.10	14.13	-25.10±0.04
Rieke and Lebofsky	80/10/9.0[3]	Infrared	J	12.75±0.07	14.38	-24.79±0.02
			H	11.83±0.06	14.26	-24.66±0.02
			K	10.92±0.03	14.13	-24.51±0.02
	80/12/9.0	Infrared	J	12.40±0.05	14.38	-24.71±.02
			H	11.54±0.04	14.26	-24.58±.02
			K	10.68±0.02	14.13	-24.44±.02
			L	9.43±0.03	13.93	-24.30±.02
			M	8.18±0.13	13.80	-24.09±.05
Dent and Balonek	79/10/25	Millimeter-Radio	89.6 GHz	1.49±0.10	10.95	-22.83±0.03
	79/10/23		31.4 GHz	1.63±0.08	10.50	-22.79±0.02
	79/10/22		2.7 GHz	2.06±0.02	9.43	-22.686±0.004
	80/9/18		89.6 GHz	1.63±0.24	10.95	-22.79±0.06
	80/9/16		31.4 GHz	2.28±0.08	10.50	-22.64±0.02
	80/10/9[4]		2.7 GHz	2.13±0.03	9.43	-22.672±0.006
	80/12/6[4]		89.6 GHz	1.74±0.24	10.95	-22.76±0.06
	80/12/6[4]		31.4 GHz	2.10±0.10	10.50	-22.68±0.02
	80/12/13		2.7 GHz	2.15±0.03	9.43	-22.668±0.006
	81/4/16		89.6 GHz	1.61±0.33	10.95	-22.79±0.09
	81/4/14		31.4 GHz	1.83±0.08	10.50	-22.74±0.02
	81/3/16[4]		2.7 GHz	2.20±0.03	9.43	-22.658±0.006
Aller, Aller, and Hodge	79/10/19[5]	Radio	14.5 GHz	2.02±0.05[6]	10.16	-22.70±0.01
			8.0 GHz	2.05±0.02[7]	9.90	-22.687±0.004
	80/10/9[5]		14.5 GHz	2.41±0.05[7]	10.16	-22.62±0.01
			8.0 GHz	2.23±0.02[7]	9.90	-22.651±0.004
			4.8 GHz	2.08±0.02	9.68	-22.681±0.004
	80/12/6[5]		14.5 GHz	2.48±0.06[8]	10.16	-22.61±0.01
			8.0 GHz	2.31±0.03[6]	9.90	-22.637±0.005
			4.8 GHz	2.22±0.02	9.68	-22.653±0.004
	81/3/26[5]		14.5 GHz	2.46±0.03	10.16	-22.61±0.01
			8.0 GHz	2.31±0.02[8]	9.90	-22.637±0.004
			4.8 GHz	2.17±0.06	9.68	-22.663±0.012

[1] Statistical errors only; calibration errors included for $\log F_\nu$.
[2] Fluxes in units of ergs $cm^{-2}\ s^{-1}$ Å^{-1}.
[3] Fluxes interpolated from measurements made on 1980 Oct 10.
[4] Interpolated from fluxes obtained more than 1 month from date.
[5] Average of fluxes obtained within 1 month of date.
[6] Three values obtained by Dent and Balonek used in the average.
[7] One value obtained by Dent and Balonek used in the average.
[8] Two values obtained by Dent and Balonek used in the average.

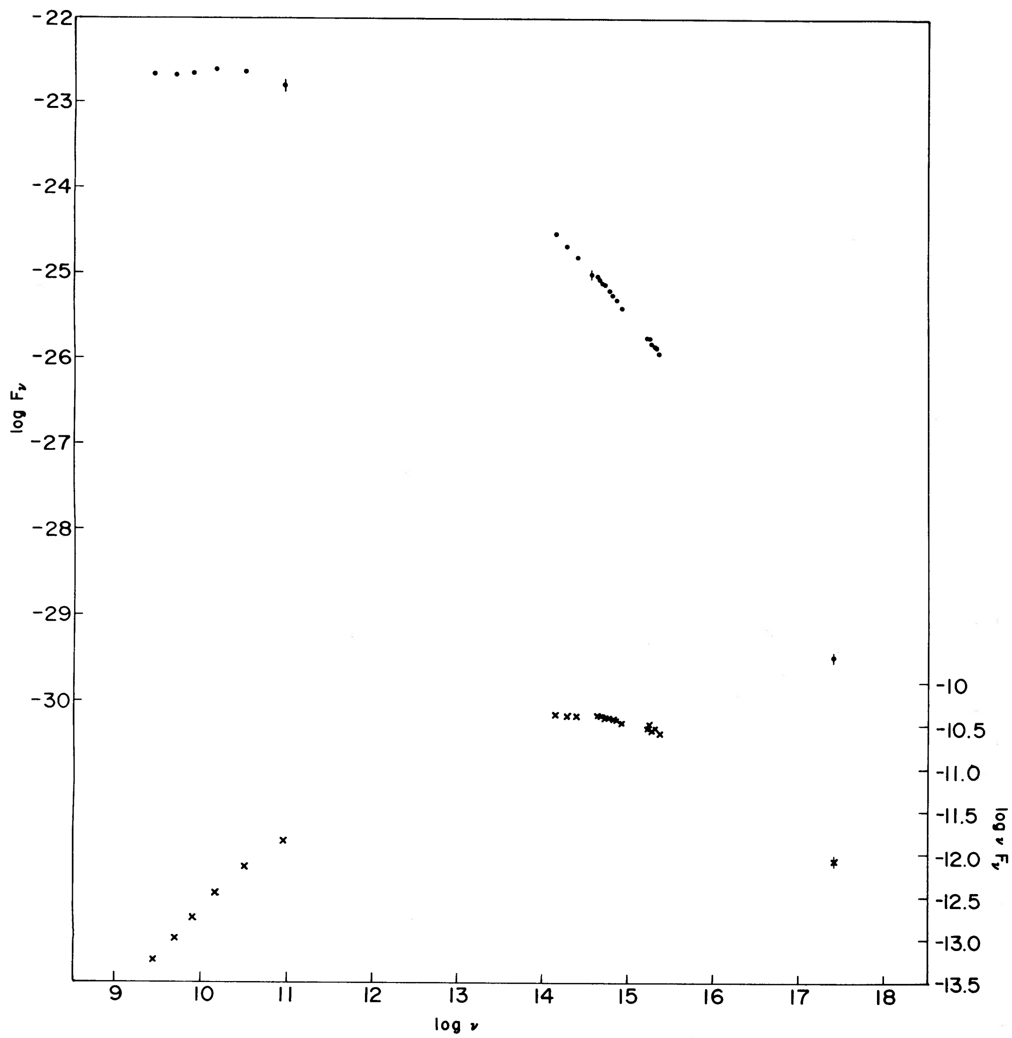

FIG. 1.—The upper curve is the multifrequency spectrum of 1980 October (log F_ν vs. log ν) corrected for reddening and plotted in the observer's frame, while the lower curve is the flux per logarithmic frequency interval (log νF_ν) as a function of frequency for the same data. Error bars less than 0.03 are not shown nor are the ultraviolet error bars (to avoid crowding). The plotted error bars are 1 sigma, except for the X-ray data, where they are approximately 2 sigma.

c) Ultraviolet Observations

Four ultraviolet spectra in the 1225–3200 Å region were obtained using the *International Ultraviolet Explorer*. The signal was extracted from the 55 line file by using the central five lines to define the signal plus background, and using the five adjacent lines (on each side) to define the background. The background lines were smoothed and filtered (11-point filter, three-point running average), and Gaussian profiles were fitted to the 15 lines perpendicular to the order at each wavelength point (de Boer, Koornneef, and Meade 1981). This procedure gives us the flux as well as its uncertainty at each wavelength point. We find no systematic differences in the flux determination between this method and the standard Goddard extraction routine.

The extracted spectra are devoid of emission lines but possess

TABLE 2

EINSTEIN X-RAY OBSERVATIONS

Date (UT)	Observer	Exposure Time (10^3 s)	$F_{0.5-3.5}$ (10^{-12} ergs cm^{-2} s^{-1})	F_1 (μJy)	Hardness Ratio
1979 Apr 8.38	CAL	2.3	1.56 ± 0.15	0.38	0.9 ± 0.3
1979 Oct 19.05	CAL	1.8	1.18 ± 0.13	0.28	1.1 ± 0.3
1980 Mar 31.72–Apr 23.14	CAL	34.6	1.24 ± 0.04	0.31	1.0 ± 0.1
1980 Oct 9.06	CFA	3.9	1.55 ± 0.12	0.34	1.0 ± 0.2
1981 Mar 26.79	CFA	4.0	1.12 ± 0.10	0.27	1.3 ± 0.2

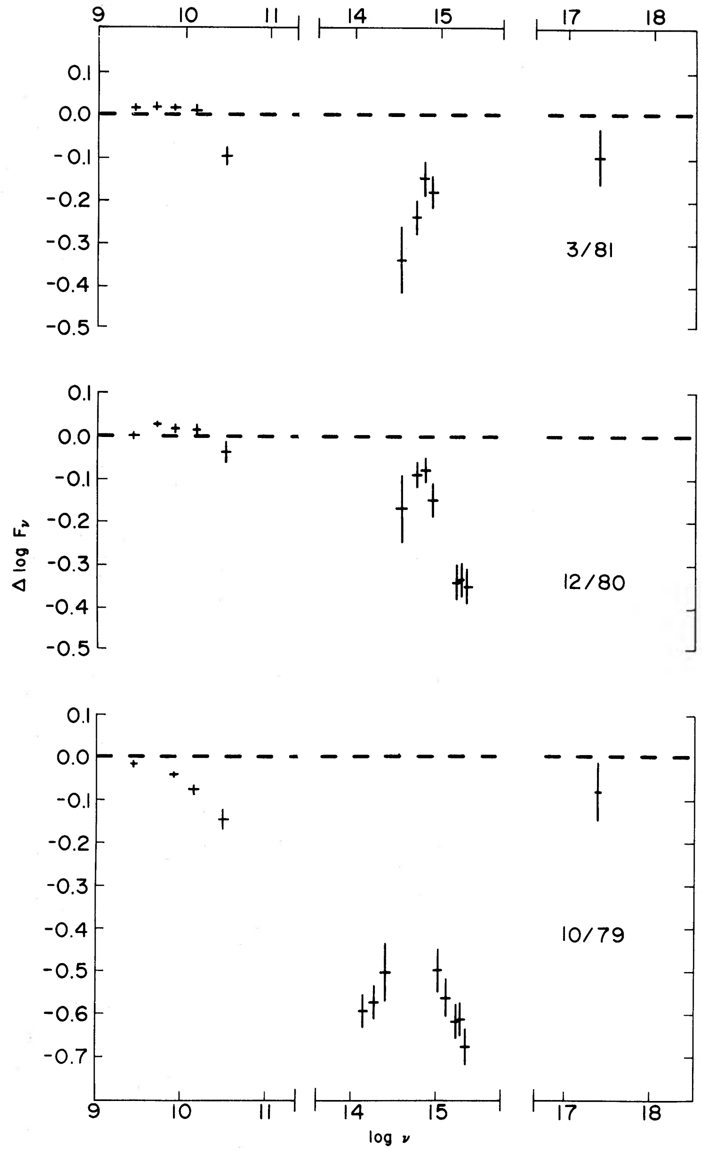

FIG. 2.—The multifrequency spectra of 1981 March (*top*), 1980 December (*middle*), and 1979 October (*bottom*) are plotted relative to the 1980 October spectrum. All plotted errors are 1 sigma, except for the X-ray data, where only the statistical errors are plotted. Because there is an additional instrumental uncertainty in the X-ray data of approximately 30% (2 sigma), there may be no differences between any of these data. Notice the small but steady increase at 2.7–15 GHz ($\log \nu = 9.43$–10.16) from 1979 October to 1980 December. Like the other radio fluxes, the 31.6 GHz flux rises between 1979 October and 1980 October but decreases by 1981 March. Variation in the IR-UV regime, which is considerably greater than at radio or X-ray frequencies, is best seen in the 1979 October data (*bottom*).

strong continuous emission against which absorption lines and continuous absorption from neutral hydrogen are seen (Bregman, Glassgold, and Huggins 1981). Excluding these absorption features, mean continuum values were determined using either 100 Å or 200 Å bins starting at 1320 Å. Although continuum flux variations greater than 15% were not found in spectra separated by 1 day during 1980 October, substantial flux variation is evident between exposures taken in 1979 October, 1980 October, and 1980 December. Relative to 1979 October, continuous emission from 0735+178 was 3.5 times brighter in 1980 October and about 1.7 times brighter in 1980 December. These variations are in strong contrast to the behavior of the X-ray emission, which is unchanged (to within 50%) during these dates. The lack of correlation in the variability at ultraviolet and X-ray frequencies suggests to us the existence of different emission processes or of separate emission regions.

The spectral slopes show weak variation between observing dates, with the spectrum being slightly steeper during 1979 October ($F_\nu \propto \nu^\alpha, \alpha = -1.76 \pm 0.08$) than during 1980 October (-1.43 ± 0.13) or 1980 October (-1.48 ± 0.15).

d) *Optical and Infrared Observations*

Photographic optical magnitudes were obtained at Rosemary Hill Observatory (University of Florida; Pica *et al.* 1980), photoelectric optical measurements were made at

TABLE 3

OPTICAL AND INFRARED VARIABILITY DURING 1980 OCTOBER

Day	Observer	*K* 14.13	*H* 14.26	*J* 14.38	*I* 14.52	*V* 14.74	*B* 14.83	*U* 14.92	α_{IR-OPT}[a]
4–5......	U. Fla.	...	...	...	...	7.7 ± 0.8	5.7 ± 0.6	...	...
5	Rieke and Lebofsky	30.2 ± 1.0	22.6 ± 0.7	16.1 ± 0.7	...	6.7 ± 0.2	5.2 ± 0.2	4.0 ± 0.1	0.99 ± 0.05
6	Rieke and Lebofsky	32.8 ± 1.0	24.3 ± 0.7	18.1 ± 0.8	14.8 ± 1.0	7.7 ± 0.2	6.0 ± 0.2	4.1 ± 0.1	0.99 ± 0.04
8–9......	U. Fla.	...	...	...	...	6.6 ± 0.6	4.3 ± 0.3	3.2 ± 0.2	...
10	Rieke and Lebofsky	29.1 ± 1.0	20.0 ± 1.2	14.1 ± 1.0	...	7.2 ± 0.2	5.4 ± 0.2	3.8 ± 0.1	0.93 ± 0.05
10–11 ...	U. Fla.	...	...	...	...	...	4.8 ± 0.5	...	...
12	Rieke and Lebofsky	...	...	...	...	6.3 ± 0.2	4.6 ± 0.2	...	...
13–14 ...	U. Fla.	...	...	...	...	...	3.3 ± 0.3	...	...
17–18 ...	U. Fla.	...	...	...	...	...	2.7 ± 0.3	...	...

NOTE.—All fluxes are in mJy.
[a] Slope determined from dereddened data.

Steward Observatory, and spectrophotometry was obtained with the image dissector scanner on the 3 m Shane telescope at Lick Observatory (Robinson and Wampler 1972). The observations reported here were made during photometric conditions, and the agreement between the different sets of data is quite good.

Monitoring studies reveal both short- and long-term optical variations. A slow increase in its average brightness occurred between 1949 and 1953 (Pollock 1974), between 1972 and 1977 (Pollock *et al.* 1979), and between 1978 and 1982 (Fig. 3*a*). Superposed upon these trends is rapid flickering in which the source changes brightness by about a magnitude on a time scale of only a few days. On the dates of the multifrequency spectra, *B* varied between 16.4 and 15.0 mag. Several sets of *UBV* observations were made in 1980 October and 1980 December during the weeks in which the multifrequency spectra were obtained. During 1980 October, these data reveal day-to-day flickering of 10%–15%, with the most rapid time scale for significant variation being 8 days (Table 3). No change in spectral slope is apparent during this period. Sporadic variation was also seen in 1980 December, when a variation of 0.5 mag was seen in data separated by 2 days, or a time scale for significant variation of approximately 5 days.

The most accurately determined optical slope of -1.27 ± 0.04 was obtained from spectrophotometry during 1980 October. Slopes derived from other optical data taken during 1980 October, 1980 December, and 1981 March are consistent with this value. This slope appears to be slightly shallower than the ultraviolet slope (Table 4).

The infrared data were taken at the Mount Lemmon facility (1979 October) and at Steward Observatory (1980 October and December). During 1980 October, the infrared measurements vary in concert with the optical data so that the infrared-optical spectrum roughly maintains its shape as it changes daily in brightness (Table 3). The best determined infrared slope of -1.01 ± 0.07, obtained during 1980 December, appears to be slightly flatter than the optical slope, but is indistinguishable from other infrared slopes (Table 4).

e) *Radio Observations*

Radio observations have been obtained at 2.7, 4.8, 7.9, 8.0, 14.5, 15.5, 31.4, and 89.6 GHz by groups at the University of Michigan and the University of Massachusetts, with four separate telescopes. The latter group regularly obtains flux measurements of 0735+178 at 2.7 GHz several times per year with the NRAO 300 ft (91 m) telescope, at 31.4 GHz and 89.6 GHz three or four times each year using the NRAO 11 m telescope at KPNO, and at 7.9 and 15.5 GHz about once per month at Haystack Observatory. At the University of Michigan, 0735+178 is observed at 4.8, 8.0, and 14.5 GHz more frequently than once per week with the 26 m paraboloid of the University of Michigan Radio Astronomy Observatory (Aller 1970; Aller, Aller, and Hodge 1981). Fluxes taken at the UMRAO and Haystack Observatory (7.9, 8.0 GHz; 14.5, 15.5 GHz) agree to within 5%.

In contrast to the optical variability, the radio data fail to show comparable day-to-day flickering, but 30% variations have been seen on a time scale of 2 months; the range of

TABLE 4

SPECTRAL SLOPES OF DEREDDENED DATA

Date	Source	$-\alpha_{IR}$	$-\alpha_{OPT}$	$-\alpha_{UV}$
1980 Dec	present work	1.01 ± 0.07	1.0 ± 0.5	1.48 ± 0.15
1980 Oct	present work	0.9 ± 0.1	1.27 ± 0.04	1.43 ± 0.13
1979 Oct	present work	0.8 ± 0.3	...	1.76 ± 0.08
1975 Oct–1978 Feb ..	O'Dell *et al.* 1978	1.0 ± 0.1 to 0.7 ± 0.2	0.9 ± 0.2 to 2.7 ± 0.4[a]	...
1975 Mar	Tapia *et al.* 1976	...	1.6 ± 0.2[a]	...
1975 Nov–1977	Rieke *et al.* 1977	0.8 ± 0.1	1.3 ± 0.1[a]	...
1975 Nov–1977	Kinman 1976	...	1.7 ± 0.1[a]	...
1975 Nov–1977	Wing 1973	...	1.8 ± 0.1[a]	...

[a] Curvature in spectrum.

1984ApJ...276..454B

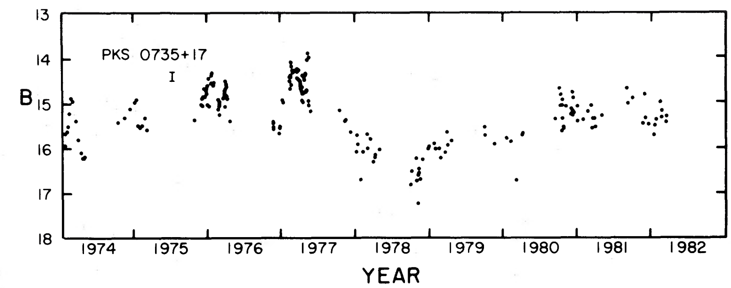

FIG. 3*a*

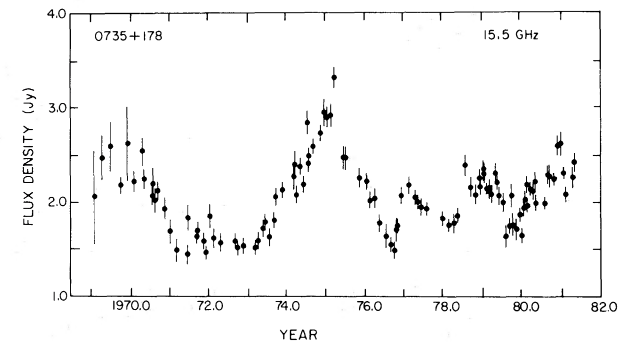

FIG. 3*b*

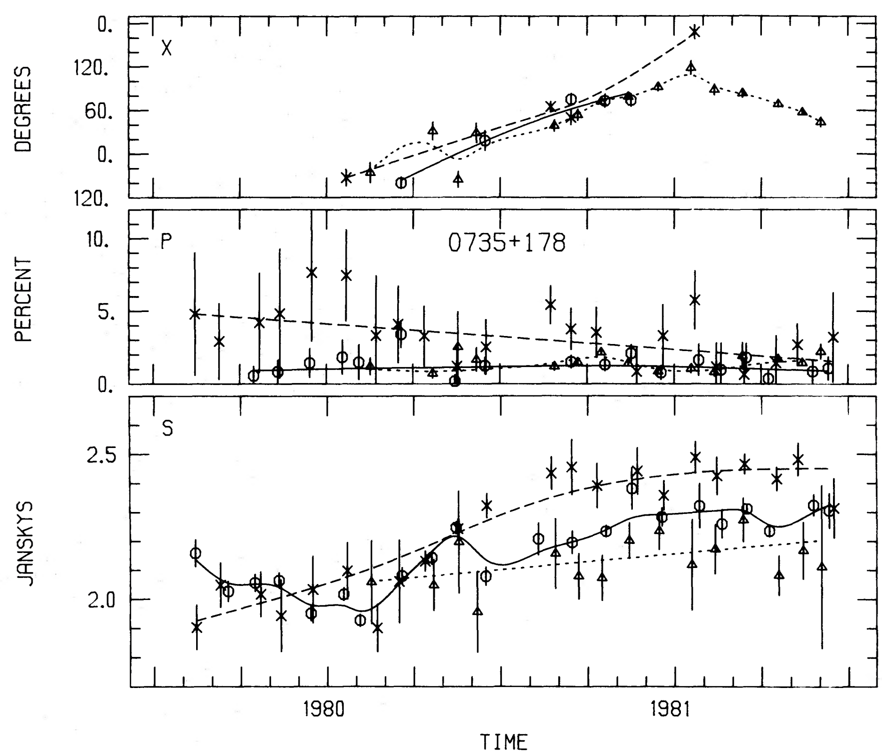

FIGS. 3*c*–3*e*

FIG. 3.—The variability in the *B* magnitude (*a*) shows rapid flickering where the brightness may change by about a magnitude in approximately a week. The flickering is superposed on long-term variation where the average *B* changes by 1–2 mag in 2–5 yr. Unlike the optical data, rapid flickering is absent in the 15.5 GHz flux variability (*b*). Here, flux variation commonly occurs on a time scale of months to years. The spectral flux (*e*), percent polarization (*d*), and polarization angle (*c*) at 4.8 GHz (△), 8.0 GHz (○), and 14.5 GHz (×) are shown for the period in which the four multifrequency spectra were obtained. Splines have been fitted to each set of data. The modest flux increases are most noticeable at 14.5 GHz, which is also the frequency of greatest polarization. The change in position angle over 180° is probably not real and may result from the 180° ambiguity in determination of polarization angle.

variability and the degree of polarization are less in the radio (Figs. 3*b*–3*e*). The radio fluxes vary considerably on a time scale of a few years (15.5 GHz), similar to the slow variation seen in the optical data. During the period when multifrequency spectra were obtained, the 2.7 GHz flux rose slowly and steadily between 1979 October and 1981 March, while the increases in the 8 and 15 GHz fluxes were larger and more rapid, reaching their highest levels at about 1980 December and maintaining this level through 1981 March (Figs. 2, 3*c*). The 31.4 GHz flux rises considerably between 1979 October and 1980 October and subsequently decreases by 1980 December and 1981 March (Fig. 2); the errors in the 89.6 GHz data are too great to make a similar comparison. The spectrum is flat from 2.7 to 15.5 GHz but always falls off slightly by 89.6 GHz. Except for the 1979 October data, the spectra defined by the 2.7–15 GHz data are slightly inverted.

III. DISCUSSION

a) *Correlated Variability*

The clear differences in the brightness variations of the various observing bands provide vital information on the nature of the emitting regions. The observations show that the X-ray flux remains essentially constant, while the IR-UV data exhibit pronounced changes of up to 350% between 1979 October and 1980 October (Table 1 and Fig. 2). During this period, the radio brightness (8–90 GHz) increased by 8%–40%, depending upon the frequency. The data show that the high-frequency radio fluxes are better correlated with the IR-UV flux than the lower frequency radio fluxes (Fig. 2), and a fuller discussion of correlated variability will appear elsewhere (Balonek and Dent 1984). Unfortunately, the absolute accuracy of the X-ray observations is insufficient to allow a useful comparison with the radio data to be made. However, because the X-rays vary slowly, if at all, and are not correlated with the IR-UV emission, we suggest that *the X-rays are produced by the inverse Compton process in the radio-emitting region* (this association is also argued for by Owen, Helfand, and Spangler 1981). Furthermore, because the IR-UV fluxes and the radio fluxes exhibit neither the same degree nor the same time scale of variability, we suggest that *the radio and X-ray emitting region is larger than the IR-UV emitting region.*

b) *Spectral Shape*

Our IR-UV data, and those of others, reveal that the spectrum of 0735+178 is time variable and often steepens with increasing frequency (Table 4). All infrared measurements ($\lambda > 1.25\ \mu$m) are consistent with a constant slope of approximately -0.9. In contrast, the optical data show evidence for wide variations in slope between -1.0 and -2.7. Ultraviolet spectral slopes are slightly steeper than infrared or optical slopes in the simultaneous spectra. Although the infrared-optical spectrum may change shape in observations separated by months or years, it retained its shape to high accuracy during a 5 day period in 1980 October when the flux varied randomly by 15% (Table 3).

If the IR-UV and the X-ray emission have separate origins (§ III*a*), then the IR-UV continuum must steepen in the energy range 1–20 rydbergs (13.6 eV–0.25 keV). The 1979 October spectrum shows that this turnover sometimes occurs in the ultraviolet because the dereddened ultraviolet data, when extrapolated to X-ray frequencies, fall significantly below the X-ray data point (3 σ effect). During 1980 October, this steepening was not observed anywhere in the IR-UV band, so the location of the turnover changes with time.

The IR-UV portions of our multifrequency spectra never connect simply to the radio data. That is, when the IR-UV spectra are extrapolated to radio frequencies, they pass far above the radio data. A flattening of the IR-UV spectrum must occur between 10^{11}–10^{14} Hz if it is to join smoothly to the radio data. One interpretation for this spectral change is that the IR-UV and radio emission are produced in the same optically thin region and from an electron distribution of complex shape. However, if this were the case, the optical and radio variability characteristics would be similar, which they are not. We suggest, as others have for other objects (e.g., Jones *et al.* 1981), that synchrotron self-absorption effects in the far-infrared range flatten the spectrum. In this hypothesis, the compact component producing the IR-UV flux is very opaque to radio photons and does not contribute significant radio emission. The radio emission must arise in a larger region of lower optical depth.

A basic test of the hypothesis that the X-rays are optically thin inverse Compton radiation is that the X-ray slope should be the same as the slope of the optically thin synchrotron photons which are scattered. We have argued (§ III*a*) that the region in which the observed IR-UV photons are produced is not the photon-scattering region. Photon scattering occurs in a larger region, probably the radio region. Unfortunately, because optical depth effects are significant in the radio region, there is no direct information on the power law of these electrons.

Most of the observed power emerges in the UV-IR regions (Fig. 1). The radio emission and the X-ray emission contribute insignificantly to the total observed power, but far-infrared emission may contribute strongly. When we connect the observations with a smooth curve, the total integrated flux during 1980 October is 3×10^{-10} ergs cm^{-2} s^{-1}, or a luminosity of 1×10^{47} ergs s^{-1} ($q_0 = 0.5$, $H_0 = 75$ km s^{-1} Mpc^{-1}, and isotropic emission assumed); variations in the total luminosity are approximately proportional to the infrared flux.

c) *Connection of the VLBI Structure with the IR-UV Observations*

VLBI observations reveal a complex multicomponent picture in which larger regions are most prominent at low frequencies, while more compact sources appear at higher frequencies (§ I). At high frequencies, the flux is concentrated in an unresolved core smaller than 0.3 mas with a 5 GHz flux of 1.1–1.3 Jy (Cotton *et al.* 1980; Bååth *et al.* 1981; Bååth *et al.* 1983) and a 30 GHz flux of 0.6 ± 0.4 Jy (this last value depends upon a deconvolution of the spectrum which is not unique). Because the emissivity at high radio frequencies is concentrated in this unresolved region, we suggest that the higher frequency IR-UV emission also arises within this region.

IV. THE PHYSICAL CONDITIONS IN THE EMITTING REGIONS

The observations (§ III) suggest a picture in which the IR-UV emission (optically thin synchrotron radiation) arises from a compact core, while the radio emission (partly opaque synchrotron radiation) and X-ray emission (inverse Compton radiation) are produced in one or more larger components.

In this section, we will adopt this picture and use theoretical models to determine the physical conditions in these regions. First, we calculate the conditions in the IR-UV region (§ IV*a*); then we derive constraints for the radial behavior of the magnetic field and particle density (§ IV*b*).

a) *Physical Conditions*

We shall estimate the conditions within the most compact emitting region, by using a modified synchrotron–self-Compton model (e.g., Jones, O'Dell, and Stein 1974) as discussed by Bregman *et al.* (1981). Briefly, a single region is characterized by one value of B, k ($dn_e/d\gamma = k\gamma^{-p}$, where n_e is the electron density, and γ is the Lorentz factor), and r, and a velocity of the emitting region with respect to the rest frame of 0735+178 (velocity toward or away from the observer only). If B and k have smooth radial dependences, this modeling will determine averages of these quantities weighted by the regions of the plasma that contribute most strongly to the optically thin synchrotron emission (the IR-UV core). The input parameters for this model are the slope in the optically thin region, the flux and frequency at which optical depth effects become important, and the flux of the inverse Compton radiation in the most compact region. Since we have argued that the inverse Compton flux comes from a larger region, we have only an upper limit to the contribution from the most compact region. The temporal flux variability size (§§ II*c*, II*d*) can be compared with the stationary model size in order to estimate the ejection velocity of the source.

The results of the modeling for various values of the turnover frequency and flux are given in Table 5. Because we have only an upper limit to the inverse Compton flux associated with the most compact region, the calculated values of B and r are formally only lower limits, and the values for k are upper limits. However, r is very weakly dependent on the inverse Compton flux ($F_{\rm iC}{}^{-0.096}$), and B is weakly dependent on it ($F_{\rm iC}{}^{-0.38}$; while $k \propto F_{\rm iC}{}^{1.1}$), so their true values are probably not very different from the lower limits. The turnover frequency is unlikely to be less than 10^{11} Hz (because self-absorption effects are already evident there) or greater than $10^{12.7}$ Hz (where the IR-UV spectrum would reach 1 Jy if extrapolated to lower frequencies). Therefore, cases 2–4 (Table 5) are most likely to be correct representations of the true situation. These calculations indicate that the magnetic field in the most compact core must be large (>0.1 G), that the size is several light weeks, and that the Lorentz factor for bulk motion of the plasma with respect to the quasar rest frame (Γ, seventh column) is less than 5. In this region, the energy densities (last three columns) of the magnetic field, photons, and particles (the most poorly determined of these quantities) are the same to within a few orders of magnitude (cases 2–4), which is suggestive of energy equipartition.

Because we do not observe directly the slope of the spectrum at the frequency where the source becomes opaque (ν_m), we have no direct knowledge of the slope of the electron spectrum there. If radiative losses affect the synchrotron spectrum in the IR-UV region, but not at ν_m, then the electron spectrum that gives rise to the emission near ν_m would be shallower by one power of the energy. If this were the case, then the density factor would be reduced by 10^3, the magnetic field would increase by 10^2, and the source size would be nearly unchanged.

The physical conditions estimated for the radio region in 0735+178 (Cotton *et al.* 1980) and other sources (e.g., Kellermann and Pauliny-Toth 1981) by using VLBI data alone yield entirely different results. The magnetic field is smaller ($10^{-4\pm1}$ G), the size is greater (10^{19}–10^{20} cm), and the energy density is entirely dominated by particles if the source is static. This supports the suggestion (§ III) that the radio-emitting region is a larger region, distinct from the IR-UV region and with different properties.

b) *Radial Behavior of the Density and Magnetic Field*

The suggestion that the X-rays are produced by the inverse Compton process in the radio region (§ III) implies that the electron-scattering depth is greater in the radio region than in the IR-UV region. Strong qualitative conclusions about the magnetic field and the density in the radio and IR-UV regions can be drawn from this inferred difference in optical depths. We illustrate this using a simplified model in which the radio and IR-UV regions are physically separate and are represented by two spherical homogeneous emitting regions of different sizes, magnetic fields, and electron densities, but with power-law electron distributions of the same index (the fundamental results are not altered by more complex models). We also assume that there is no motion of one region relative to the other. In this model, which is suggested by the observations (§ III), the larger region becomes opaque to its synchrotron radiation at a lower frequency than the small region. Consequently, the large region dominates the radio emission, while the small region dominates the IR-UV emission (Fig. 4). The X-ray emission is primarily produced in the large region by the inverse Compton scattering of its own synchrotron photons, or those from the smaller region. Finally, we must apply the basic principles of synchrotron and inverse Compton emission to complete this model.

The optically thin synchrotron spectral flux S from a source at some frequency is related to the radius r, magnetic field B,

TABLE 5

PHYSICAL CONDITIONS IN THE MOST COMPACT REGION

Model No.	$\log \nu_m$ (Hz)	F_m (Jy)	r (cm)	B (G)	k (cm^{-3})	Γ	u_B (ergs cm^{-3})	u_P (ergs cm^{-3})[a]	$u_{\rm PH}$ (ergs cm^{-3})
1	10.7	1	1.7(17)	0.06	2.7(6)	5.8	1.0(−4)	7.0(−2)	6.0(−4)
2	11.2	1	9.0(16)	0.8	2.8(6)	3.2	3.0(−2)	8.0(−2)	2.0(−2)
3	11.7	1	4.7(16)	13	3.0(6)	1.7	7.0	8.0(−2)	1.0
4	12.2	1	2.6(16)	180	3.0(6)	1.2	1.0(3)	8.0(−2)	3.0(1)
5	12.7	1	1.4(16)	2400	3.0(6)	1.0	2.0(5)	8.0(−2)	1.0(3)

[a] Particle energy density computed for a minimum electron energy of $30m_e c^2$.

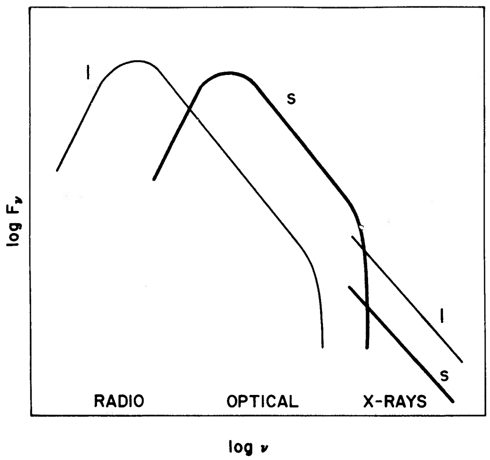

FIG. 4.—Diagram of emission from a large (l) and small (s) emitting region. Synchrotron emission from the large region dominates the radio emission, while synchrotron emission from the smaller region gives rise to the optical emission. The inverse Compton radiation from the large region is primarily responsible for the X-ray emission.

spectral index for optically thin radiation α, and the electron density factor k ($\alpha = -[p - 1]/2$) by the relationship

$$S = Cr^3kB^{1-\alpha} , \qquad (1)$$

where C is a constant. The inverse Compton spectral flux that is produced by scattering of a region's own synchrotron photons is (D is a constant)

$$F_{\mathrm{iC}} = Dr^4k^2B^{1-\alpha} , \qquad (2)$$

whereas the inverse Compton spectral flux produced by a larger region scattering synchrotron photons from a smaller region is

$$F_{\mathrm{iC}} = D(rk)_l(r^3kB^{1-\alpha})_s , \qquad (3)$$

where l and s refer to the large and small regions, respectively. Together with equations (1)–(3), we use the conditions that the small region dominates the optically thin synchrotron emission ($S_l < S_s$), and that the large region is the primary contributor to the X-ray spectral flux ($F_l > F_s$), to establish the *strong quantitative conditions*

$$(rk)_l > (rk)_s \quad \text{and} \quad (r^2B^{1-\alpha})_s > (r^2B^{1-\alpha})_l . \qquad (4)$$

These inequalities are valid independently of whether the source photons are from the radio or the IR-UV region (which may be separated in space from the radio region). In the latter case, a dilution factor must be included in equation (3), and the inequalities, equation (4), become stronger. For 0735+178, equation (4) means that *the magnetic field is diminished in the radio region relative to its value in the IR-UV region.* Also, if the lower energy limit to the electron distribution in the large region is the same or less than that in the small region, *the mass of emitting plasma in the radio region is greater than in the IR-UV region.* If this analysis were applied to the case where k and B vary smoothly in radius between the two regions, we would conclude that k decreases less rapidly than r^{-1}, and B decreases more rapidly than $r^{-2/(1-\alpha)}$ (e.g., r^{-1} for $\alpha = -1$).

Independent information about the radial behavior of B and k is provided by the flatness of the radio continuum. For a source whose density factor and magnetic field vary smoothly in radius as

$$dn_e/d\gamma = k(r)\gamma^{-p} , \quad \text{where} \quad k(r) = k_0(r/r_0)^{-n} ; \qquad (5a)$$

$$B = B_0(r/r_0)^{-m} , \qquad (5b)$$

the slope of the continuum when the optical depth effects are important is (e.g., Marscher 1977)

$$\alpha_{\mathrm{thick}} = \frac{[3m + 5n + 2p(m - 1) - 13]}{[2n + m(p + 2) - 2]} . \qquad (6)$$

The flat radio spectrum ($\alpha_{\mathrm{thick}} = 0$), the slope of the optically thin flux ($\alpha = -1$, $p = 3$), and the inequalities derived above (eq. [4]) restrict the range of m and n. Upon making the assumption that the density factor is a decreasing function of radius ($n > 0$), then $19/9 > m > 14/9$ and $1 > n > 0$. The latter inequality implies that the density factor k decreases in radius less rapidly than has been suggested by dynamical models ($n > 2$, e.g., Pacholczyk 1981). Naturally, k must eventually decrease more rapidly than r^{-3} to prevent the emitting region from having infinite mass.

We note that it is impossible for us to exclude other explanations for the origin of the X-ray flux (e.g., thermal emission); in which case, the arguments presented above do not apply.

V. SUMMARY

The multifrequency spectra obtained here for 0735+178 have been powerful tools for determining the properties in the continuum-emitting plasma. A more complete understanding of this region has been developed by analyzing these spectra together with our variability data, existing VLBI data, and theoretical models. We find that the continuum-emitting region is broken into at least two parts. Optically thin synchrotron radiation from the smaller region dominates the IR-UV emission; most of the observed power comes from here. In this region, the radius, magnetic field, and density parameter k are approximately 5×10^{16} cm, 1–100 G, and $\sim 10^6$ cm^{-3}, respectively. In the larger region, partly optically thick emission dominates the radio flux, while inverse Compton radiation may give rise to the X-ray emission. Although this region contributes little to the total observed power, it probably contains more mass in emitting plasma than the IR-UV region. The radio observations are reproduced, and theoretical constraints are satisfied if the radius, magnetic field, and density parameter in this region are 10^{18}–10^{20}, $\sim 10^{-3}$ G, and $\sim 10^4$–10^6 cm^{-3}. The Lorentz factor of the relativistic motion of the emitting region toward the observer is probably 1.2–3. The particle energy density, which may not be far from equipartition with the photon and magnetic field densities in the IR-UV region, is dominant in the radio and X-ray region(s) provided the bulk Lorentz factor of this region is not large.

The support and kind assistance of a number of telescope assistants and data reduction personnel made these observations possible. Special thanks are extended to D. Helfand and M. Elvis for their role in scheduling certain X-ray observations. In addition, financial support was provided to: the University of Florida monitoring program through a series of grants from the NSF (current grant AST 820 3926); the UMRAO from the

NSF; G. H. R. and M. J. L. from the NSF; the Haystack Observatory from the NSF; the Columbia Astrophysical Laboratory from NASA; D. A. S. from NASA; J. M. from the NSF; and J. N. B., and A. E. G., and P. J. H. from NASA. The NRAO is operated by Associated Universities, Inc., under contract to the NSF.

REFERENCES

Aller, H. D. 1970, *Ap. J.*, **161**, 1.
Aller, H. D., Aller, M. F., and Hodge, P. E. 1981, *A.J.*, **86**, 325.
Angel, J. R. P., and Stockman, H. S. 1980, *Ann. Rev. Astr. Ap.*, **18**, 321.
Bååth, L. B., *et al.* 1983, in press.
Bååth, L. B., Elgered, G., Lundqvist, G., Graham, D., Weiler, K. W., Seielstad, G. A., Tallqvist, S., and Schilizzi, R. T. 1981, *Astr. Ap.*, **96**, 316.
Balonek, T. 1982, Ph.D. thesis, University of Massachusetts.
Balonek, T., and Dent, W. A. 1984, in preparation.
Boksenberg, A., Carswell, R. F., and Sargent, W. L. W. 1979, *Ap. J.*, **227**, 370.
Bregman, J. N., *et al.* 1982, *Ap. J.*, **253**, 19.
Bregman, J. N., Glassgold, A. E., and Huggins, P. J. 1981, *Ap. J.*, **249**, 13.
Bregman, J. N., Lebofsky, M. J., Aller, M. F., Rieke, G. H., Aller, H. D., Hodge, P. E., Glassgold, A. E., and Huggins, P. J. 1981, *Nature*, **293**, 714.
Burstein, D., and Heiles, C. 1978, *Ap. J.*, **225**, 40.
Carswell, R. F., Strittmatter, P. A., Williams, R. E., Kinman, T. D., and Serkowski, K. 1974, *Ap. J.* (*Letters*), **190**, L101.
Cotton, W. D., *et al.* 1980, *Ap. J.* (*Letters*), **238**, L123.
de Boer, K. S., Koornneef, J., and Meade, M. R. 1981, in *The Universe at Ultraviolet Wavelengths: The First Two Years of International Ultraviolet Explorer*, ed. R. D. Chapman (NASA CP-2171), p. 771.
Glassgold, A. E., *et al.* 1983, *Ap. J.*, **274**, 101.
Heiles, C. 1975, *Astr. Ap. Suppl.*, **20**, 37.
Hewitt, A., and Burbidge, G. 1980, *Ap. J.*, **43**, 57.
Impey, C. D., Brand, P. W. J. L., Wolstencroft, R. D., and Williams, P. M. 1982, *M.N.R.A.S.*, **200**, 19.
Jones, T. W., O'Dell, S. L., and Stein, W. A. 1974, *Ap. J.*, **188**, 353.
Jones, T. W., Rudnick, L., Owen, F. N., Puschell, J. J., Ennis, D. J., and Werner, M. W. 1981, *Ap. J.*, **243**, 97.
Kellermann, K. I., and Pauliny-Toth, I. I. K. 1981, *Ann. Rev. Astr. Ap.*, **19**, 373.
Kinman, T. D. 1976, *Ap. J.*, **205**, 1.
Marscher, A. P. 1977, *A.J.*, **82**, 781.
Marscher, A. P., and Shaffer, D. B. 1980, *A.J.*, **85**, 668.
O'Dell, S. L., Puschell, J. J., Stein, W. A., and Warner, J. W. 1978, *Ap. J. Suppl.*, **38**, 267.
Owen, F. N., Helfand, D. J., and Spangler, S. R. 1981, *Ap. J.* (*Letters*), **250**, L55.
Pacholczyk, A. G. 1981, *Ap. Letters*, **21**, 87.
Perley, R. A. 1982, *A.J.*, **87**, 859.
Pica, A. J., Pollock, J. T., Smith, A. G., Leacock, R. J., Edwards, P. L., and Scott, R. L. 1980, *A.J.*, **85**, 1442.
Pollock, J. T. 1974, *Ap. J.* (*Letters*), **198**, L53.
———. 1982, Ph.D. thesis, University of Florida.
Pollock, J. T., Smith, A. G., Leacock, R. J., Edwards, P. L., and Scott, R. L. 1979, *A.J.*, **84**, 1658.
Puschell, J. J., and Stein, W. A. 1980, *Ap. J.*, **237**, 331.
Rieke, G. H., Lebofsky, M. J., Kemp, J. C., Coyne, G. V., and Tapia, S. 1977, *Ap. J.* (*Letters*), **218**, L37.
Robinson, L. B., and Wampler, E. J. 1972, *Pub. A.S.P.*, **84**, 161.
Sargent, W. L. W., Young, P. J., Boksenberg, A., and Tytler, D. 1980, *Ap. J. Suppl.*, **42**, 41.
Seaton, M. J. 1979, *M.N.R.A.S.*, **187**, 73P.
Tapia, S., Craine, E. R., and Johnson, K. 1976, *Ap. J.*, **203**, 291.
Tolbert, C. R. 1972, *Astr. Ap. Suppl.*, **3**, 349.
Ulvestad, J. S., Johnston, K. J., and Weiler, K. W. 1982, *Ap. J.*, **266**, 18.
Weymann, R. J., Williams, R. E., Peterson, B. M., and Turnshek, D. A. 1979, *Ap. J.*, **234**, 33.
Wing, R. F. 1973, *A.J.*, **78**, 684.
Zamorani, G., *et al.* 1981, *Ap. J.*, **245**, 357.

H. D. ALLER, M. F. ALLER, and P. E. HODGE: Department of Astronomy, University of Michigan, 953 Physics-Astronomy Building, Ann Arbor, MI 48109

T. J. BALONEK: Hopkins Observatory, Department of Physics and Astronomy, Williams College, Williamstown, MA 01267

J. N. BREGMAN, A. E. GLASSGOLD, and P. J. HUGGINS: Physics Department, New York University, 4 Washington Place, New York, NY 10003

W. A. DENT: Department of Physics and Astronomy, GR Tower B, University of Massachusetts, Amherst, MA 01003

W. H.-M. KU: Columbia Astrophysics Laboratory, Columbia University, New York, NY 10027

R. J. LEACOCK, A. J. PICA, A. G. SMITH, and J. WEBB: Department of Astronomy, University of Florida, Gainesville, FL 32611

M. J. LEBOFSKY, G. H. RIEKE, and R. J. RUDY: Steward Observatory, University of Arizona, Space Sciences Building, Tucson, AZ 85721

P. D. LEVAN: AFFGL/OPI, Hanscom AFB, MA 01931

J. S. MILLER: Lick Observatory, University of California, Santa Cruz, CA 95064

C. P. O'DEA: NRAO, Edgemont Road, Charlottesville, VA 22901

J. T. POLLOCK: Astronomy Department, Villanova University, Villanova, PA 19085

D. A. SCHWARTZ: Center for Astrophysics, 60 Garden Street, Cambridge, MA 02138